Catalysis Science & Technology

Accepted Manuscript

This article can be cited before page numbers have been issued, to do this please use: X. Jia, J. Ma, M. wang, X. Li, J. gao and J. Xu, *Catal. Sci. Technol.*, 2016, DOI: 10.1039/C6CY00874G.

This is an *Accepted Manuscript*, which has been through the Royal Society of Chemistry peer review process and has been accepted for publication.

Accepted Manuscripts are published online shortly after acceptance, before technical editing, formatting and proof reading. Using this free service, authors can make their results available to the community, in citable form, before we publish the edited article. We will replace this *Accepted Manuscript* with the edited and formatted *Advance Article* as soon as it is available.

You can find more information about *Accepted Manuscripts* in the Information for Authors.

Please note that technical editing may introduce minor changes to the text and/or graphics, which may alter content. The journal's standard Terms & Conditions and the Ethical guidelines still apply. In no event shall the Royal Society of Chemistry be held responsible for any errors or omissions in this *Accepted Manuscript* or any consequences arising from the use of any information it contains.

ROYAL SOCIETY OF CHEMISTRY

www.rsc.org/catalysis

View Article Online
DOI: 10.1039/C6CY00874G

Catalysis Science & Technology

ARTICLE

Alkali α-MnO_2/Na_xMnO_2 collaboratively catalyzed ammoxidation-Pinner tandem reaction of aldehydes

Received 00th January 20xx,
Accepted 00th January 20xx

DOI: 10.1039/x0xx00000x

www.rsc.org/

Xiuquan Jia,[a,b] Jiping Ma,*[a] Min Wang,[a] Xiaofang Li,[a,b] Jin Gao[a] and Jie Xu*[a]

Tandem reaction is a growing field to yield important advances towards green and sustainable chemistry. We report a bifunctional manganese oxides catalyst with interface binding redox phase (α-MnO_2) and basic phase (Na_xMnO_2). The molar ratio of NaOH/Mn plays great role on the formation of α-MnO_2/Na_xMnO_2. Sodium cation is essential for formation of a basic Na_xMnO_2 phase while potassium cation promotes to form a redox active a-MnO_2 phase. The interface structure of α-MnO_2/Na_xMnO_2 geometrically favors the ammoxidation-Pinner tandem reaction to synthesize imidates with 58-96% yields from aldehydes. The phase collaborative effect is observed. In the ammoxidation process, the redox cycle of Mn^{IV}/Mn^{III} is involved and the lattice oxygen in α-MnO_2 phase acts as active oxygen species. The O-H in methanol is activated and dissociated on the basic sites of Na_xMnO_2 to adsorbed methoxyl species to facilitate Pinner synthesis. This approach bypasses conventional synthesis of imidates suffering from harsh reaction conditions and multiple steps.

1. Introduction

New methodologies to assemble complex synthetic sequences in a tandem reaction are great impetus to atom economy, overall process simplicity, as well as biomimetic catalysis.[1] Traditionally, more than one catalyst is used to promote two or more mechanistically distinct reaction steps. The reaction intermediate has to diffuse from the first catalyst site to the next. If the distances are too large, concentration gradients develop and catalytic activity as well as selectivity decreases.[2] In comparison to the composite solid catalysts with isolated components, a nanoscale integrated structure with different functionalities is a promising candidate for tandem reactions owing to the close geometry of multicatalytic functions and favor for collaborative catalysis.[3] However, the fabrication of high catalytic efficiency with nanoscale intimacy of different functionalities is still challenging owing to the lack of deep understanding of the physical-chemical features of the catalyst and difficulty in accommodating mechanistically different catalytic cycles under the same reaction condition.[4]

Manganese oxides are characterized by versatile crystal structures and tunable redox and acid-base properties.[5] Recently, manganese oxides interface was developed by integrating different structures to form a composite in which the two components are connected by a structurally compatible close-packed oxygen array.[6] By tailoring the composition of the crystal structures of manganese oxides, two or more distinct functionalities could be located in an interfacial manner and collaboratively catalyze the tandem reaction.

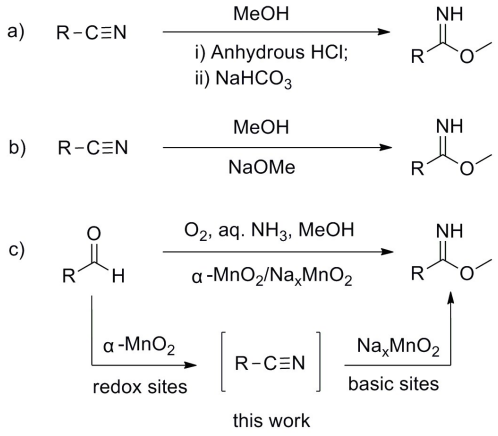

Scheme 1 The methods for the synthesis of imidates.

Imidate is an important class of nitrogen-containing motif in the chemistry and biology.[7] It is traditionally obtained through Pinner synthesis in the presence of hazardous hydrogen chloride gas, or strong base using nitrile as substrate (Scheme 1a, b), and was barely reported to be synthesized though a single tandem reaction from more readily available aldehydes (Scheme 1c), owing to 1) the easily decomposed or hydrolyzed properties of imidates at high temperature;[8] 2) the generally inert reactivity for ammoxidation at low temperature; 3) the insufficient acid or base catalysts for nitrile addition with alcohol. We challenge the conventional wisdom of the rules by fabricating a manganese oxides catalyst with nanoscale intimacy of redox and base functionalities for ammoxidation

[a] State Key Laboratory of Catalysis, Dalian Institute of Chemical Physics, Chinese Academy of Sciences, Dalian National Laboratory for Clean Energy, Dalian 116023, P. R. China. E-mail: xujie@dicp.ac.cn; majiping@dicp.ac.cn.
[b] University of the Chinese Academy of Sciences, Beijing 100049, P. R. China.
†Electronic Supplementary Information (ESI) available: See DOI: 10.1039/x0xx00000x

and nitrile addition, respectively. Very recently, Manganese oxide based octahedral molecular sieves (KMn_8O_{16}; OMS-2) was found to be efficient catalysts for ammoxidation at low temperature by our group.[9] However, OMS-2 was not an effective catalyst for the Pinner reaction. A major challenge needed in this reasearch is to develop catalytic sites for Pinner reaction. To date, no example exists for the heterogeneously catalytic addition reaction of nitrile with methanol. Herein, on the basis of our previous work,[9,10] we demonstrate the active manganese oxides integrating redox phase (α-MnO_2) and basic phase (Na_xMnO_2) for efficiently catalyzing the ammoxidation-Pinner tandem reaction. When α-MnO_2 and Na_xMnO_2 are combined in a physical mixture, the initial ammoxidation step and the further Pinner reaction could not efficiently occur concurrently. In contrast, the nanoscale co-existence of the two forms of manganese oxides in a single material was found to be vital to the success of the tandem reaction. This approach allows for the synthesis of various imidates from aldehydes under ambient conditions. The phase boundary collaborative effect is observed. The parameters effect on the formation of α-MnO_2/Na_xMnO_2, the reaction route and the activation of substrate as well as intermediates on the α-MnO_2/Na_xMnO_2 were studied in detail.

2. Experimental

2.1 Materials

All chemicals were of analytical grade and used as received unless otherwise stated. MeOH, aq. NH_3, Fe_2O_3, Co_3O_4, NiO, TiO_2, ZrO_2, WO_3, CuO, $KMnO_4$, $MnSO_4$ and $MnCl_2$ were purchased from Tianjin Kermel Chemical Reagent Co. Ltd.. Furfural, 5-methylfurfural, 3,4-dimethylfurfural, 5-bromo-furfural, 5-phenylfurfural, pyridine-2-carboxaldehyde, pyridine-4-carboxaldehyde, 3-nitrobenzaldehyde, 4-nitro-benzaldehyde, p-chlorobenzaldehyde, p-hydroxybenzaldehyde, anisic aldehyde, cinnamaldehyde, isobutyraldehyde, Nb_2O_5, CeO_2, MgO and Mn_3O_4 were obtained from Aladdin Chemistry Co. Ltd.. V_2O_5 is domestic reagent. 5-Iodofurfural, thiophen-2-carboxaldehyde, 4-bromothiophen-2-carboxaldehyde, 2-furonitrile and 2-furamide were purchased from TCI Shanghai. 5-Ethylfurfural, benzofurfural and γ-MnO_2 were obtained from Alfa Aesar. 5-Ethoxymethylfurfural was purchased from Sigma-Aldrich. α-MnO_2,[11] β-MnO_2,[12] δ-MnO_2,[13] OMS-2[14] and Na_xMnO_2[15] were prepared according to the literature procedures.

2.2 Catalyst preparation

The α-MnO_2/Na_xMnO_2 catalyst used in this work was prepared by coprecipitation method. In a typical preparation, the calculated amounts of $KMnO_4$ (40 mmol) and NaOH (120 mmol) was dissolved in 100 mL deionized water. The obtained solution was added into another 100 mL aqueous solution of $Mn(NO_3)_2$ (60 mmol). After stirring at room temperature for 4 h, the resulting solid, where the molar ratio of added NaOH to the total Mn salts (NaOH/Mn) is 1.2, was collected by filtration, washed repeatedly with distilled water, and finally dried overnight in air at 60 °C, then calcined in air at desired temperature for 4 h. The preparation procedure of α-MnO_2/Na_xMnO_2 with different molar ratio of NaOH/Mn is the same as α-MnO_2/Na_xMnO_2 with NaOH/Mn molar ratio of 1.2 except that different amount of NaOH was used.

2.3 Catalyst characterization

The X-ray powder diffraction (XRD) patterns were obtained using Rigaku D/Max 2500/PC powder diffractometer with Cu Kα radiation (λ = 0.15418 nm) at 40 kV and 200 mA in a scanning rate of 5 °/min. High-resolution transmission electron microscopy (HRTEM) was performed with a JEOL JEM-2100EM microscope. The samples were suspended in ethanol with an ultrasonic dispersion for 5−10 min, and then a few droplets of the suspension were put on a microgrid carbon polymer supported on a copper grid and allowed to dry at room temperature for TEM observations. CO_2 temperature programmed desorption (CO_2-TPD) was conducted using a Micromeritics Autochem 2910. The catalyst sample was pretreated in Ar for 1.5 h at 200 °C. After cooling to 50 °C in Ar, Pulse CO_2 adsorption was performed until peaks are equal or 20 times. The temperature was increased from 50 to 800 °C at a rate of 10 °C min^{-1} under pure He flow. The evolved gas analysis was performed using a quadrupole mass spectrometer (Ominstar 300). Electron paramagnetic resonance (EPR) was performed on a Bruker spectrometer in the X-band at room temperature with a field modulation of 100 kHz. The microwave frequency was maintained at 9.401 GHz. The X-ray photoelectron spectroscopy (XPS) measurements were performed on a Thermo ESCALAB 250Xi spectrometer equipped with a monochromated AlKα X-ray source (hυ = 1486.6 Ev, 15 kV, 10.8 mA). The samples were vacuum dried at 120 °C for 12 h. The charge neutralizer system was used for all of the analyses. The base pressure was 1×10^{-8} Pa. High resolution spectra were recorded with 20-eV pass energy. The pass energies correspond to the $Ag3d_{5/2}$ FWHM of 0.65 eV. The data were acquired with 0.05 eV steps. The binding energy (BE) was calibrated to the C1*s* signal (284.6 eV) as a reference. The curve fitting procedure was performed using an approximation based on a combination of the Gaussian and Lorentzian functions with subtraction of a Shirley-type background. In situ Fourier transform infrared spectroscopy (FT-IR) spectra of methanol adspecies on catalysts were recorded with a TENSOR 27 spectrometer equipped with an in situ IR cell, which was connected to a conventional gas flow system. The samples (20-30 mg) were pressed into a self-supporting wafer (20 mm diameter) and mounted into the IR cell. Adsorption of methanol was carried out in the following method: The sample was used without pretreatment. Methanol was fed to the in situ IR cell under vacuum (< 10^{-1} Pa). Then, the IR disk was purged with N_2, and IR measurement was carried out until the spectrum was stable.

2.4 Determination of *H*_ of Na_xMnO_2

The base strength of the sample was detected by a series of Hammett indicators.[16] The indicators included phenolphthalein (*H*_ = 9.3), 2,4-dinitroaniline (*H*_ = 15.0), 4-nitroaniline (*H*_ = 18.4), benzidine (*H*_ = 22.5), 4-chloroaniline (*H*_ = 26.5), and aniline (*H*_ = 27.0). The sample was transferred to purified benzene. Two drops of indicator solution (0.1 wt % indicator dissolved in benzene) were added to the suspension, and the color change of the indicator was monitored visually.

2.5 Catalytic activity test

Catalytic reactions were performed in a 20 mL stainless steel autoclave equipped with a magnetic stirrer, a pressure gauge, and automatic temperature control apparatus. The reactor was connected to an oxygen cylinder for reaction pressure. In a typical experiment, furfural (48.0 mg, 0.5 mmol), aq. NH_3 (120 μL, 3 equiv.), MeOH (5 mL) and α-MnO_2/Na_xMnO_2 prepared with NaOH/Mn molar ratio of 1.2 and calcined at 250 °C (0.1 g) were loaded into the reactor. After sealing and charging with O_2 (0.5 MPa), the autoclave was heated to the desired temperature (30 °C). After reaction, the autoclave was cooled. The solution was separated by centrifugation and analyzed by GC using the internal standard method. A larger scale transformation of furfural (0.24 g, 2.5 mmol; 5-fold scale) was carried out for product isolation. After reaction, the solution was separated by centrifugation. MeOH was removed by rotary evaporator and dichloromethane (15 mL) was added. The resulting solution was washed with brine (3 × 5 mL) and dried by anhydrous sodium sulfate. The product was obtained after evaporation of dichloromethane. Other isolated products were obtained under similar experimental conditions.

2.6 Products analysis

The products were identified by Agilent 6890N GC/5973MS as well as by comparison with the retention times to corresponding standards in GC traces. Gas chromatography measurements were conducted on Agilent 7890A GC with autosampler and a flame ionization detector. HP-5 capillary column (30 m × 530 μm × 1.5 μm) was used for separation of reaction mixtures. The temperature of the column was initially kept at 100 °C for 5 min, and then was increased at a rate of 20 °C min^{-1} to 220 °C and kept for 10 min. The conversion of furfural and yield of corresponding products were evaluated using 1,3,5-trimethylbenzene as the internal standard. The conversion of other substrates and selectivity of corresponding products were determined based on area normalization without any purification.

3. Results and discussion

3.1 Structure of α-MnO_2/Na_xMnO_2

The α-MnO_2/Na_xMnO_2 was prepared the same with α-MnO_2 except that NaOH was added in the mixture of $KMnO_4$ and $Mn(NO_3)_2$, where the molar ratio of added NaOH to the total Mn salts (NaOH/Mn) is 1.2. The as-prepared materials were thermally treated at different temperatures under air to modulate the activity of redox and basic sites. The crystal structure was characterized by X-ray powder diffraction (XRD) (Fig. 1A). At low calcination temperature, the crystallinity is poor and only the peaks attributed to α-MnO_2 (JCPDS#00-044-0141) phase are observed. As calcination temperature increases, the crystallinity improves. When the calcination temperature is above 420 °C, the characteristic {002} diffraction peak of layered Na_xMnO_2 (JCPDS#00-027-0751) at around 2θ of 15.8° also appears.[15] The diffraction peak of possible segregation of potassium manganate species K_xMnO_2 (JCPDS#00-030-0951) was not observed.

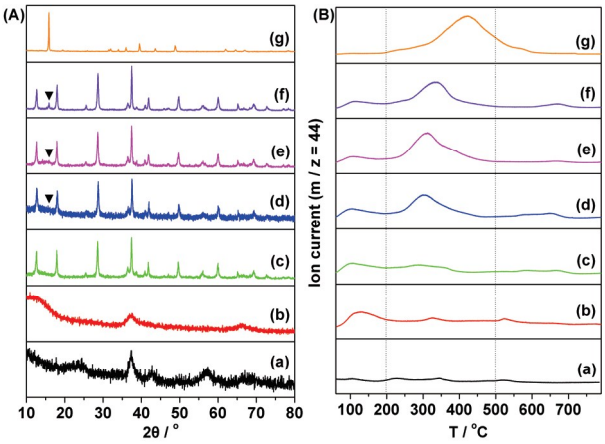

Fig. 1 (A) XRD patterns (B) CO_2-TPD profiles of α-MnO_2 (a), α-MnO_2/Na_xMnO_2 with NaOH/Mn molar ratio of 1.2 calcined at 250 °C (b), 400 °C (c), 420 °C (d), 450 °C (e), 500 °C (f) and Na_xMnO_2 (g).

The co-existence of α-MnO_2 and Na_xMnO_2 is directly observed by the high-resolution transmission electron microscopy (HRTEM) (Fig. 2 and Fig. S7). α-MnO_2 {110} crystal plane with lattice spacing of 0.69 nm and Na_xMnO_2 {002}[17] crystal plane with lattice spacing of 0.57 nm were observed and in close proximity which may geometrically favor the collaborative catalysis in the nanoscale.

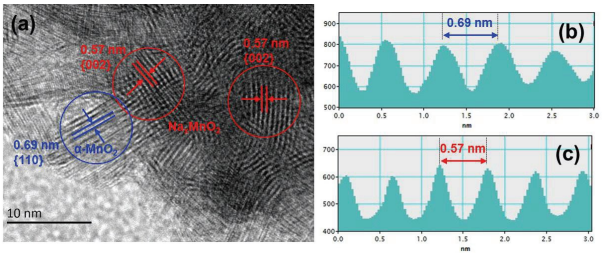

Fig. 2 HRTEM image of α-MnO_2/Na_xMnO_2 with NaOH/Mn molar ratio of 1.2 calcined at 450 °C (a), and the corresponding crystal lattice space of α-MnO_2 {110} (b) and Na_xMnO_2 {002} (c).

The parameters effect on the formation of α-MnO_2/Na_xMnO_2 were further investigated. The molar ratio of NaOH/Mn is of significance for the formation of α-MnO_2/Na_xMnO_2. The co-existence of α-MnO_2 and Na_xMnO_2

was just detected when the molar ratio of NaOH/Mn was more than 1.08. While the co-existence of α-MnO_2 and Mn_2O_3 (JCPDS#00-024-0508) was detected when the molar ratio of NaOH/Mn was less than 1.08. Other Mn^{II} salts such as $MnSO_4$, $MnCl_2$, $Mn(OAc)_2$ has no obvious influence on the formation of MnO_2/Na_xMnO_2. The co-existence of α-MnO_2 and Mn_2O_3 was detected when substituting KOH for NaOH. $KMnO_4$ was also replaced with $NaMnO_4$ to prepare the catalyst under the identical condition. Unexpectedly, the crystal strucure has changed completely. The peaks attributed to α-MnO_2 could not be obviously detected (Fig. S8), indicating that the crystalline structures of a-MnO_2 could no longer be stabilized in the absence of potassium ions. Induced coupling plasma elemental analysis results (Table S5) imply that the obtained manganese oxide is another type of compound, which is quite different from α-MnO_2/Na_xMnO_2.

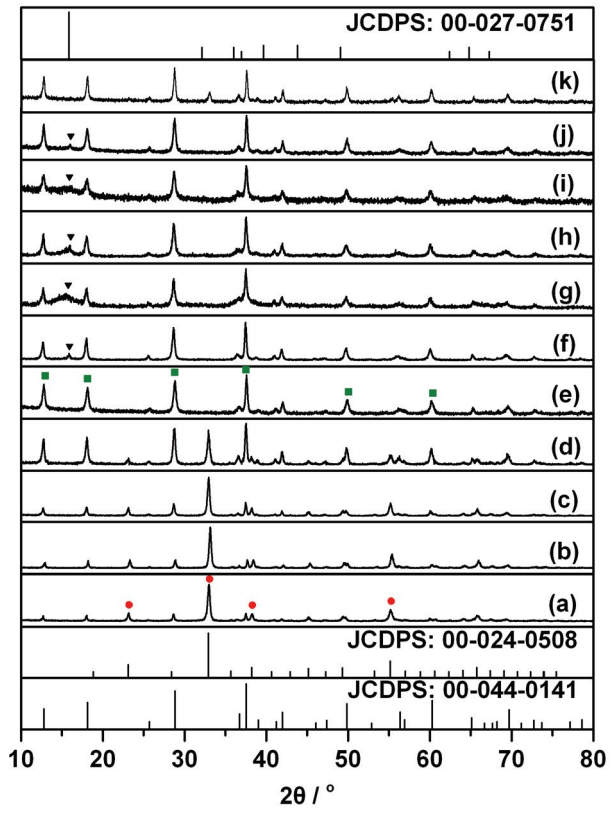

Fig. 3 XRD patterns of manganese oxides calcined at 500 °C with NaOH/Mn molar ratio of 0 (a), 0.24 (b), 0.60 (c), 0.96 (d), 1.08 (e), 1.2 (f), 1.8 (g), 1.2 and substituting $MnSO_4$ for $Mn(NO_3)_2$ (h), 1.2 and substituting $MnCl_2$ for $Mn(NO_3)_2$ (i), and 1.2 and substituting $Mn(OAc)_2$ for $Mn(NO_3)_2$ (j) , and 1.2 and substituting KOH for NaOH (k).

3.2 Basicity of α-MnO_2/Na_xMnO_2

We employed CO_2 temperature programmed desorption (CO_2-TPD) to probe the surface basicity of manganese oxides (Fig. 1B). α-MnO_2/Na_xMnO_2 with NaOH/Mn molar ratio of 1.2 calcined at different temperatures all show a CO_2 desorption peak at temperature range of 200-500 °C which is attributed to the moderate basic sites. The base density of α-MnO_2/Na_xMnO_2 calcined at 250 °C is 6.0 × 10^{-4} mmol m^{-2} which is 20 times more than that of α-MnO_2 (0.3 × 10^{-4} mmol m^{-2}) and OMS-2 (0.4 × 10^{-4} mmol m^{-2}). Furthermore, Na_xMnO_2 was found to possess abundant amount of basicity (4.5 × 10^{-3} mmol m^{-2}) with strength 9.3 <*H*< 15.0. These results indicate that the basicity on the surface of α-MnO_2/Na_xMnO_2 is ascribed to the Na_xMnO_2 phase. To explore the possible role of potassium cation on the generation of basicity, we synthesized the catalyst with KOH instead of NaOH. The obtained manganese oxides possess little basicity (0.06 × 10^{-4} mmol m^{-2}), indicating that the basicity is not caused by potassium cation.

3.3 Catalytic performance of α-MnO_2/Na_xMnO_2

Table 1. Catalytic conversion of furfural over different manganese oxides.[a]

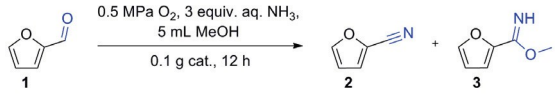

Entry	Catalyst	Conv. (%)	Yield (%)	
			2	**3**
1[b]	blank	90	-	-
2	α-MnO_2	> 99	91	5
3	β-MnO_2	> 99	67	19
4	γ-MnO_2	> 99	49	43
5	δ-MnO_2	> 99	33	17
6	OMS-2	> 99	86	8
7	Na_xMnO_2	87	2	2
8[c]	α-MnO_2 + Na_xMnO_2	> 99	83	13
9[d]	α-MnO_2 + Na_xMnO_2	> 99	17	80
10[e]	α-MnO_2/Na_xMnO_2	> 99	11	89

[a]Reaction conditions: 0.5 mmol furfural, 0.1 g catalyst, 120 μL aq. NH_3 (3 equiv.), 5 mL MeOH, 0.5 MPa O_2, 30 °C, 12 h. [b]Only aldimine was detected by GC. [c]0.08 g α-MnO_2 and 0.02 g Na_xMnO_2 were physical mixed. [d]*0.1 g* α-MnO_2 and 0.12 g Na_xMnO_2 were physical mixed. [e]α-MnO_2/Na_xMnO_2 refers to α-MnO_2/Na_xMnO_2 with NaOH/Mn molar ratio of 1.2 calcined at 250 °C thereafter unless otherwise stated.

Initially, we selected biomass-derived furfural as a model substrate for ammoxidation-Pinner tandem reaction. V_2O_5, Fe_2O_3, NiO, Mn_3O_4, TiO_2, Nb_2O_5, ZrO_2, WO_3, CeO_2, MgO, and CuO were used as catalyst but nearly no ammoxidation product was observed (Fig. S10). Previously, we used OMS-2 as catalyst for the ammoxidation of 5-hydroxymethylfurfural in methanol. The *in situ* generated cyano group in the presence of electron-withdrawing substituent is exceptionally active to further react with methanol without additional catalyst.[9] Herein, however, OMS-2 mainly offers ammoxidation product of 2-furonitrile (Table1, entry 6), showing the generally robust property of unactivated cyano group. Other manganese dioxides, such as β-MnO_2, δ-MnO_2, γ-MnO_2 and α-MnO_2, give 33%-91% yield of 2-furonitrile, together with a low yield (5%-43%) of methyl furan-2-carboximidate (Table 1, entries 2-5). α-MnO_2 shows the highest yield of 2-furonitrile (91% yield)

but lowest yield of methyl furan-2-carboximidate (5% yield) (Table 1, entry 2). It is probable that α-MnO_2 possesses highly active redox sites and few basic sites. Na_xMnO_2 showed high activity for the addition of 2-furonitrile with methanol (Fig. 9B), but nearly no ammoxidation reaction happened with furfural as initial substrate (Table 1, entry 7). It could be due to the poor redox properties of Na_xMnO_2.

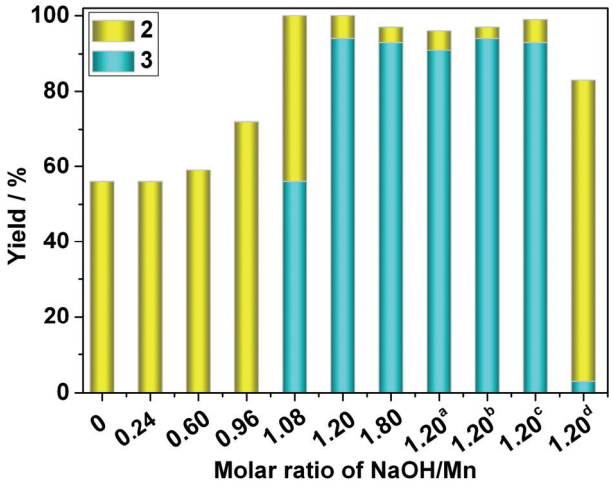

Fig. 4 Catalytic conversion of furfural over α-MnO_2/Na_xMnO_2 with different molar ratio of NaOH/Mn calcined at 500 °C. Reaction conditions: 0.5 mmol furfural, 0.1 g catalyst, 120 μL aq. NH_3 (3 equiv.), 5 mL MeOH, 0.5 MPa O_2, 30 °C, 12 h. [a] Substituting $MnSO_4$ for $Mn(NO_3)_2$. [b] Substituting $MnCl_2$ for $Mn(NO_3)_2$. [c] Substituting $Mn(OAc)_2$ for $Mn(NO_3)_2$. [d] Substituting KOH for NaOH.

Then the ammoxidation-Pinner tandem reactions were carried out over the different phase-structured manganese oxide-based catalysts presented in Fig. 3, and the catalyst structure-activity relationships are shown in Fig. 4. All of these manganese oxides can truly catalyze the aerobic ammoxidation reaction at 30 °C. However, the Pinner addition activities of these samples are quite different. The samples with the co-existence of α-MnO_2 and Mn_2O_3 (NaOH/Mn ratio less than 1.08) have no addition activities on in situ generated nitriles, whereas the samples with the co-existence of α-MnO_2 and Na_xMnO_2 (NaOH/Mn ratio more than 1.08) show efficient addition activity. It is only the united α-MnO_2/Na_xMnO_2 phase that is responsible for the considerable enhancement in the redox-base catalytic activity for the ammoxidation-Pinner tandem reaction.

Furthermore, the physical mixture of α-MnO_2 and Na_xMnO_2 were tested for the ammoxidation-Pinner tandem reaction (Table 1, entry 8-9; Fig. 5). As shown in Fig. 5, high yield of 2-furonitrile and low yield of methyl furan-2-carboximidate were maintained when Na_xMnO_2 was the minor composition. With increasing the molar fraction of Na_xMnO_2, the total yield of 2-furonitrile and methyl furan-2-carboximidate decreased, indicating the ammoxidation efficiency was decreased. The optimization of molar ratio of α-MnO_2 to Na_xMnO_2 gave the best imidate yield of 36%. To obtain a high level of imidate product over the physical mixture of the catalysts, additional Na_xMnO_2 should be added without decreasing the amount of α-MnO_2 (Table 1, entry 9). In comparison, α-MnO_2/Na_xMnO_2, with co-existence of redox phase of α-MnO_2 and basic phase of Na_xMnO_2 in an interfacial manner, shows both high activity and selectivity for the methyl furan-2-carboximidate (Table 1, entry 10). These results indicate that the nanoscale co-existence of α-MnO_2 and Na_xMnO_2 favors the phase collaborative catalysis.

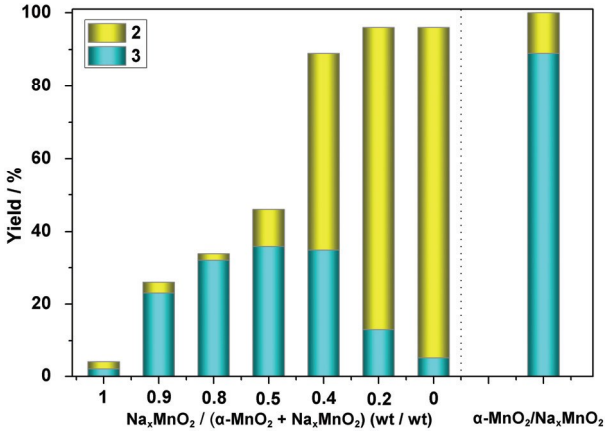

Fig. 5 Catalytic conversion of furfural over different manganese oxides. Reaction conditions: 0.5 mmol furfural, 0.1 g catalyst, 120 μL aq. NH_3 (3 equiv.), 5 mL MeOH, 0.5 MPa O_2, 30 °C, 12 h. α-MnO_2 + Na_xMnO_2 refers to α-MnO_2 and Na_xMnO_2 physical mixed.

The tandem synthesis of imidate is very sensitive to temperature. Amide becomes the major product when the temperature is above 90 °C. Moreover, the total yields of the products are also decreased (Table S1, entries 2 and 3).

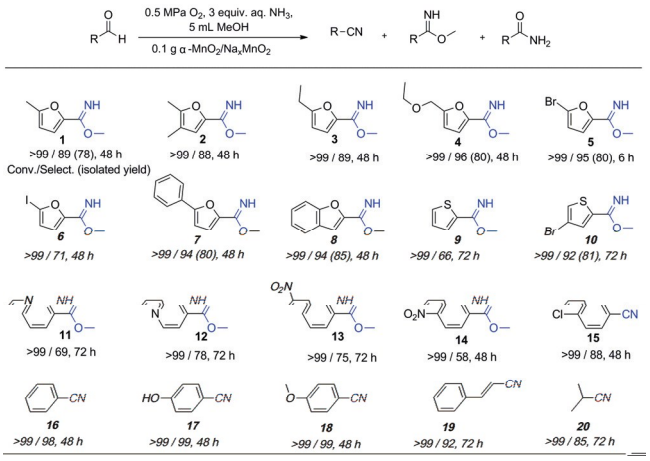

Fig. 6 Catalytic conversion of aryl aldehydes to imidates. Reaction conditions: 0.5 mmol substrate, 0.1 g α-MnO_2/Na_xMnO_2, 120 μL aq. NH_3 (3 equiv.), 5 mL MeOH, 0.5 MPa O_2, 30 °C. The data in bracket is isolated yield.

α-MnO_2/Na_xMnO_2 is an efficient catalyst for the tandem synthesis of a wide range of imidates. Furfural derivatives, thienyl and pyridyl aldehydes were converted to the corresponding imidates in 66-96% yields (Fig. 6, entries 1-12). Furfural with electron-withdrawing substituent of Br- can

provide a high level of imidate product in 6 h; even in the case of using OMS-2 as catalyst, the corresponding imidate was effectively generated (Scheme S1). An evident substituent effect is also observed for phenyl aldehydes. Except for NO_2-substituted benzaldehydes, nitriles were the major products for Cl-, HO-, H-, MeO- substituted benzaldehydes and non-aromatic aldehyde (Fig. 6, entries 13-20).

3.4 Kinetic study

The time course of methyl furan-2-carboximidate synthesis over α-MnO_2/Na_xMnO_2 was investigated (Fig. 7). Firstly, aldimine was generated and oxidized rapidly to 2-furonitrile. The volcano curves for both aldimine and 2-furonitrile indicate that they are reaction intermediates. Methyl furan-2-carboximidate gradually increased to 94% yields after 30 h. These results demonstrate that the tandem reaction proceeds by three consecutive steps: 1) the aldimine formation from furfural; 2) the ammoxidation of the aldimine group to cyano group; 3) the imidate formation via the addition reaction of cyano group with methanol.

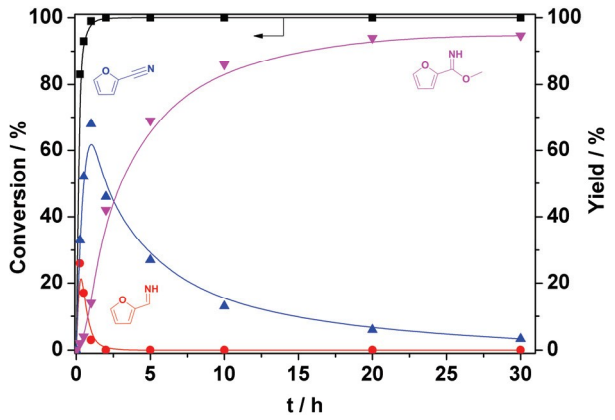

Fig. 7 Time course of catalytic conversion of furfural to methyl furan-2-carboximidate over α-MnO_2/Na_xMnO_2 (■ = conversion of **1**, ● = yield of aldimine, ▲ = yield of **2**, ▼ = yield of **3**. Reaction conditions: 3 mmol furfural, 0.6 g α-MnO_2/Na_xMnO_2, 720 μL aq. NH_3 (3 equiv.), 30 mL MeOH, 0.5 MPa O_2, 30 °C.

3.5 Mechanism of ammoxidation-Pinner tandem reaction

We then studied the reaction mechanism of ammoxidation step. Only aldimine was obtained without α-MnO_2/Na_xMnO_2 under 0.5 MPa O_2 (Table 1, entry 1). On the other hand, the reaction can take place without oxygen in the presence of α-MnO_2/Na_xMnO_2. The total yields of the products increased with increasing α-MnO_2/Na_xMnO_2 amount (Fig. S11). 82% yield of imidate was obtained with 12 equivalents of α-MnO_2/Na_xMnO_2[17] (Eq.1).

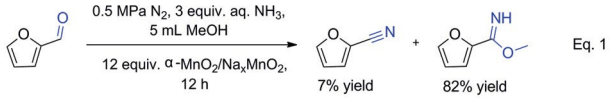

Eq. 1

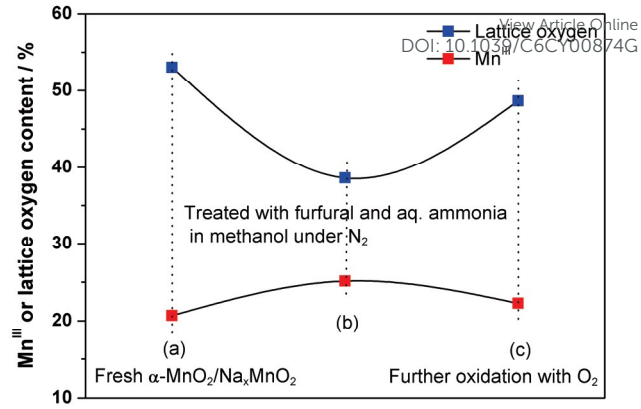

Fig. 8 The changes of lattice oxygen and Mn^{III} content derived from XPS spectra. (a) fresh α-MnO_2/Na_xMnO_2, (b) α-MnO_2/Na_xMnO_2 was treated with furfural and ammonia in MeOH at 30 °C under N_2 atmosphere for 48 h, (c) α-MnO_2/Na_xMnO_2 in (b) was treated at 30 °C under O_2 atmosphere for 12 h.

The changes of surface oxygen on α-MnO_2/Na_xMnO_2 were studied by O1s X-ray photoelectron spectroscopy (XPS) (Fig. S12A and Fig. 8). The peaks at 529.5 eV and 531.2 eV are ascribed to the surface lattice oxygen (O_{latt}) species and adsorbed oxygen (O_{ads}) species, respectively.[18] Quantitative analysis shows the content of surface O_{latt} first decreases from 53% to 39% upon treating with furfural and ammonia in methanol under N_2 atmosphere, and then restores to 49% after further treatment under O_2 atmosphere. These results demonstrate that ammoxidation step is a Mars–van-Krevelen reaction[19] where aldimine is oxidized to nitrile, and the lattice oxygen is consumed and subsequently restored by molecular oxygen.

The changes of surface lattice oxygen are accompanied by the variation of Mn valence, which were further investigated by electron paramagnetic resonance (EPR) characterization (Fig. S13). A nearly symmetric single line is a feature common to all MnO_2 samples. The broad line width (ΔH) is caused by Mn^{III} species.[20] After α-MnO_2/Na_xMnO_2 was treated with furfural and ammonia in methanol under N_2 atmosphere, the ΔH broadens from 241 mT to 318 mT (Fig. S13a, b), and then returns to 205 mT after further treatment with O_2 (Fig. S13c). These results demonstrate that Mn^{IV} was reduced to a relatively high fraction of Mn^{III} by the substrate under N_2 atmosphere, and then Mn^{III} was oxidized back to Mn^{IV} by O_2, leading to a low fraction of Mn^{III}. This result is in agreement with the changes of Mn^{III} content monitored by XPS characterization (Fig. S12B and Fig. 8).

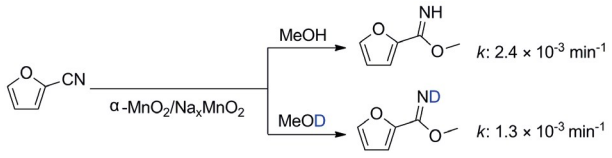

Scheme 2 Kinetic isotopic effects (KIE) for 2-furonitrile addition with methanol.

The mechanism of basic sites-catalyzed addition step was further investigated. The addition reaction of 2-furonitrile with methanol should involve O-H bond dissociation step. A large

value of k_H/k_D (1.8) at 30 °C indicates that the dissociation of the O-H bond in the methanol is the kinetically-relevant step for addition reactions (Scheme 2).

In situ CH_3OH adsorption Fourier transform infrared spectroscopy (FT-IR) characterization was carried out to study the activation of methanol over α-MnO_2/Na_xMnO_2. Methanol on KBr flake shows three C-O stretching vibrations bands with P, Q and R branches centering at 1016, 1033 and 1055 cm^{-1}, respectively (Fig. 9A).[21] By contrast, the Q and P braches disappear after methanol adsorbing on α-MnO_2/Na_xMnO_2, owing to the restriction effect on the rotation of *C* axis by dissociative adsorption. Furthermore, a red shift of R branch from 1055 to 1030 cm^{-1} is observed, indicating the weakening of C-O bond. The addition rate is linearly increased with surface moderate base density (Fig. 9B). These results demonstrate that the basic sites in α-MnO_2/Na_xMnO_2 catalyze the O-H bond dissociation and subsequent formation of metal-methoxy species.

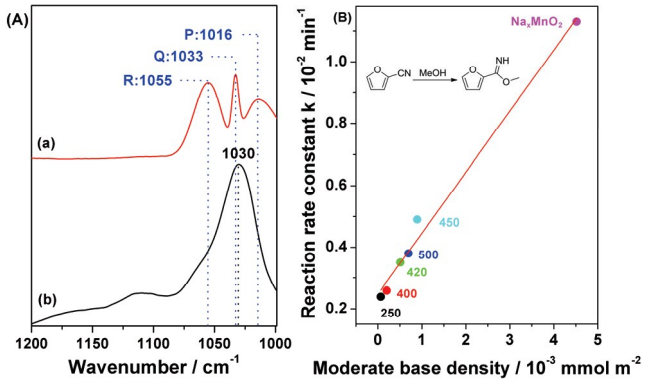

Fig. 9 (A) FT-IR spectra of adsorbed MeOH on KBr (a) and α-MnO_2/Na_xMnO_2 (b). (B) The dependence of addition reaction rate constant *k* on the moderate base density of α-MnO_2/Na_xMnO_2 calcined at different temperatures or Na_xMnO_2. Reaction condition: 1 mmol 2-furonitrile, 0.05 g α-MnO_2/Na_xMnO_2 or Na_xMnO_2, 10 mL MeOH, 30 °C.

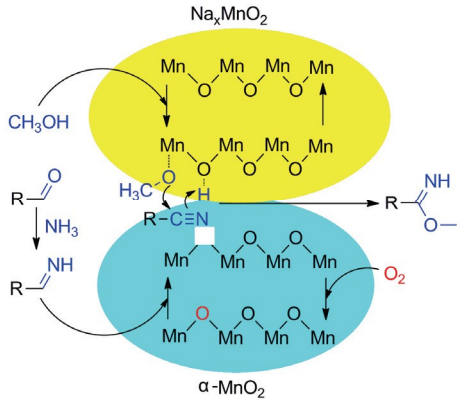

Scheme 3. Proposed reaction mechanism for the tandem reaction over α-MnO_2/Na_xMnO_2.

Based on the above results, a reaction mechanism is tentatively proposed (Scheme 3). Firstly, aldehdye reacts with NH3 to form aldimine intermidate which is subsequently fast oxidized to nitrile on the redox sites of α-MnO_2 phase. In the oxidation process, Mn^{IV} is reduced to Mn^{III} and one lattice oxygen is consumed. The lattice oxygen is restored by the molecular oxygen. Methanol is activated by the basic sites on the Na_xMnO_2 phase. O-H is dissociated to form adsorbed methoxyl species, which attacks the nitrile to form imidate. The interface structure of α-MnO_2/Na_xMnO_2 binds the activated methoxyl and nitrile in close proximity and geometrically favors the addition reaction.

Conclusions

In summary, the α-MnO_2/Na_xMnO_2 catalyst with co-existence of redox and substantial basicity functionalities in an interface manner was found to be an efficient and reusable heterogeneous catalyst for tandem synthesis of imidates with 58-96% yields from aldehydes and aqueous ammonia in the presence of methanol under ambient conditions. The molar ratio of NaOH/Mn plays great role on the formation of α-MnO_2/Na_xMnO_2. Sodium cation is essential for formation of a basic Na_xMnO_2 phase while potassium cation does not afford basic phases. On the other hand, potassium cation promotes to form a redox active a-MnO_2 phase by incorporated into its tunnel structure while sodium cation can not. Application of two kinds of alkali metal cations in the synthesis of the catalysts is the key point for obtaining active catalysts for the tandem reaction. The interface structure of α-MnO_2/Na_xMnO_2 geometrically favors the tandem reaction. Ammoxidation of aldehydes to nitriles happens on the redox phase of α-MnO_2 and subsequent addition of nitrile intermediates with methanol occurs on the basic sites of Na_xMnO_2. The phase collaborative effect is observed.

Acknowledgements

This work was supported by the National Natural Science Foundation of China (projects 21233008 and 21303183) and the "Strategic Priority Research Program-Climate Change: Carbon Budget and Related Issues" of the Chinese Academy of Sciences (XDA05010203).

Notes and references

1 (a) T. L. Lohr and T. J. Marks, *Nat. Chem.*, 2015, **7**, 477-482; (b) M. C. Haibach, S. Kundu, M. Brookhart and A. S. Goldman, *Acc. Chem. Res.*, 2012, **45**, 947-958; (c) M. J. Climent, A. Corma, S. Iborra and M. J. Sabater, *ACS Catal.*, 2014, **4**, 870-891.

2 (a) J. Francis, E. Guillon, N. Bats, C. Pichon, A. Corma and L. Simon, *Appl. Catal. A - Gen.*, 2011, **409**, 140-147; (b) J. Kim, W. Kim, Y. Seo, J.-C. Kim and R. Ryoo, *J. Catal.*, 2013, **301**, 187-197.

3 (a) J. Zecevic, G. Vanbutsele, K. P. de Jong and J. A. Martens, *Nature*, 2015, **528**, 245-248; (b) Y. Yang, X. Liu, X. Li, J. Zhao, S. Bai, J. Liu and Q. Yang, *Angew. Chem. Int. Ed.*, 2012, **124**, 9298-9302; (c) J. Graciani, K. Mudiyanselage, F. Xu, A. E. Baber, J. Evans, S. D. Senanayake, D. J. Stacchiola, P. Liu, J. Hrbek and J. F. Sanz, *Science*, 2014, **345**, 546-550.

4 (a) J. Lu, J. Dimroth and M. Weck, *J. Am. Chem. Soc.*, 2015, **137**, 12984-12989; (b) D. C. Leitch, J. A. Labinger and J. E. Bercaw, *Organometallics*, 2014, **33**, 3353-3365.

View Article Online
DOI: 10.1039/C6CY00874G

5 (a) Z. Chen, Z. Jiao, D. Pan, Z. Li, M. Wu, C.-H. Shek, C. L. Wu and J. K. Lai, *Chem. Rev.*, 2012, **112**, 3833-3855; (b) J. Hou, Y. Li, L. Liu, L. Ren and X. Zhao, *J. Mater. Chem. A*, 2013, **1**, 6736-6741; (c) Z.-R. Tian, W. Tong, J.-Y. Wang, N.-G. Duan, V. V. Krishnan and S. L. Suib, *Science*, 1997, **276**, 926-930; (d) K. Yamaguchi, H. Kobayashi, Y. Wang, T. Oishi, Y. Ogasawara and N. Mizuno, *Catal. Sci. Technol.*, 2013, **3**, 318-327; (e) V. Duffort, E. Talaie, R. Black and L. F. Nazar, *Chem. Mater.*, 2015, **27**, 2515-2524.

6 (a) S. Guo, H. Yu, P. Liu, X. Liu, M. Chen, M. Ishida and H. Zhou, *J. Mater. Chem. A*, 2014, **2**, 4422-4428; (b) M. M. Thackeray, S.-H. Kang, C. S. Johnson, J. T. Vaughey, R. Benedek and S. Hackney, *J. Mater. Chem.*, 2007, **17**, 3112-3125; (c) C. Johnson, N. Li, J. Vaughey, S. Hackney and M. Thackeray, *Electrochem. Commun.*, 2005, **7**, 528-536.

7 (a) R. Roger and D. G. Neilson, *Chem. Rev.*, 1961, **61**, 179-211; (b) M. E. Voss, C. M. Beer, S. A. Mitchell, P. A. Blomgren and P. E. Zhichkin, *Tetrahedron*, 2008, **64**, 645-651; (c) K.-S. Yeung, M. E. Farkas, J. F. Kadow and N. A. Meanwell, *Tetrahedron Lett.*, 2005, **46**, 3429-3432; (d) R. P. Frutos, X. Wei, N. D. Patel, T. G. Tampone, J. A. Mulder, C. A. Busacca and C. H. Senanayake, *J. Org. Chem.*, 2013, **78**, 5800-5803; (e) Y. Donde and L. E. Overman, *J. Am. Chem. Soc.*, 1999, **121**, 2933-2934; (f) M. Noè, A. Perosa and M. Selva, *Green Chem.*, 2013, **15**, 2252-2260; (g) G. S. Leoung, D. W. Feigal, A. B. Montgomery, K. Corkery, L. Wardlaw, M. Adams, D. Busch, S. Gordon, M. A. Jacobson, P. A. Volberding and D. Abrams, *N. Engl. J. Med.*, 1990, **323**, 769-775; (h) R. R. Tidwell, S. K. Jones, J. D. Geratz, K. A. Ohemeng, M. Cory and J. E. Hall, *J. Med. Chem.*, 1990, **33**, 1252-1257. (i) K. Popov, A. Hoang and P. Somfai, *Angew. Chem. Int. Ed.*, 2016, **55**, 1801–1804.

8 (a) T. Okuyama, T. C. Pletcher, D. J. Sahn and G. L. Schmir, *J. Am. Chem. Soc.*, 1973, **95**, 1253-1265; (b) D. J. Gavin and C. A. Mojica, *Org. Process Res. Dev.*, 2001, **5**, 659-664.

9 X. Jia, J. Ma, M. Wang, H. Ma, C. Chen and J. Xu, *Green Chem.*, 2016, **18**, 974-978.

10 (a) J. Ma, Z. Du, J. Xu, Q. Chu and Y. Pang, *ChemSusChem*, 2011, **4**, 51-54; (b) X. Jia, J. Ma, M. Wang, Z. Du, F. Lu, F. Wang and J. Xu, *Appl. Catal. A - Gen.*, 2014, **482**, 231-236; (c) J. Cai, H. Ma, J. Zhang, Q. Song, Z. Du, Y. Huang and J. Xu, *Chem. Eur. J.*, 2013, **19**, 14215-14223; (d) Z. Du, J. Ma, F. Wang, J. Liu and J. Xu, *Green Chem.*, 2011, **13**, 554-557;

11 E. Schleitzer, *Gmelin Handbook of Inorganic Chemistry 8th Edition (Manganese)*, Verlag Chemie GmbH, Weinheim/Bergstrasse, 1973.

12 F. Y. Cheng, T.R. Zhang, Y. Zhang, J. Du, X. P. Han, J. Chen, *Angew. Chem. Int. Ed.*, 2013, **52**, 2474-2477.

13 O. Ghodbane, J.-L. Pascal and F. Favier, *ACS Appl. Mater. Interfaces.*, 2009, **1**, 1130-1139.

14 R. N. DeGuzman, Y.-F. Shen, E. J. Neth, S. L. Suib, C.-L. O'Young, S. Levine and J. M. Newsam, *Chem. Mater.*, 1994, **6**, 815-821.

15 R. Stoyanova, D. Carlier, M. Sendova-Vassileva, M. Yoncheva, E. Zhecheva, D. Nihtianova, C. Delmas, *J. Solid State Chem*. 2010, **183**, 1372-1379.L. B. Sun, F. N. Gu, Y. Chun, J. Yang, Y. Wang and J. H. Zhu, *J. Phys. Chem. C*, 2008, **112**, 4978-4985.

16 J. P. Parant, Olazcuag.R, Devalett.M, Fouassie.C and Hagenmul.P, *J. Solid State Chem.*, 1971, **3**, 1-11.

17 The molar mass of α-MnO_2/Na_xMnO_2 was approximate to that of MnO_2.

18 F. J. Shi, F. Wang, H. X. Dai, J. X. Dai, J. G. Deng, Y. X. Liu, G. M. Bai, K. M. Ji and C. T. Au, *Appl. Catal. A-Gen.*, 2012, **433**, 206-213.

19 H. D. Noether, *J. Chem. Phys.*, 1942, **10**, 693-699.

20 M. Kakazey, N. Ivanova, Y. Boldurev, S. Ivanov, G. Sokolsky, J. Gonzalez-Rodriguez and M. Vlasova, *J. Power Sources*, 2003, **114**, 170-175.

21 H. D. Noether, *J. Chem. Phys.*, 1942, **10**, 693-699.

Journal Name ARTICLE

View Article Online
DOI: 10.1039/C6CY00874G

Graphical abstract

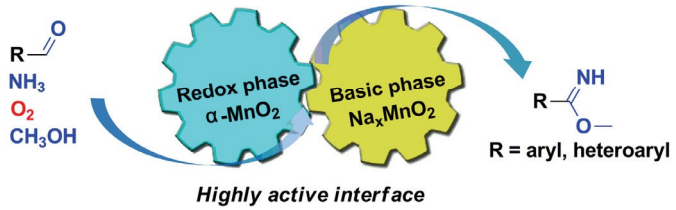

A bifunctional manganese oxide catalyst with interface binding redox phase (α-MnO_2) and basic phase (Na_xMnO_2) was reported for the ammoxidation-Pinner tandem reaction to synthesize imidates with 58-96% yields from aldehydes.